Molecular Mobility in Para-Substituted Polyaryls. 2. Glass Transition Phenomena in Amorphous Poly(aryl ether ether ketone)

L. David* and S. Etienne

INSA, Groupe d'Etude de Métallurgie Physique et de Physique des Matériaux, U.A. CNRS 341, Bât. 502, 20 av. A. Einstein, 69621 Villeurbanne Cedex, France

Received August 13, 1992; Revised Manuscript Received March 20, 1993

ABSTRACT: The dynamic mechanical behavior of amorphous poly(aryl ether ether ketone) has been investigated and analyzed in the frame of a model involving quasi punctual defects (QPD model). Accordingly, the molecular motions responsible for the glass transition are cooperative and hierarchically constrained through series correlated processes. The Kolhrausch exponent of the relaxation function is identified with a correlation parameter b and is explicitly related to the microstructural state through the QPD's concentration Cd. In the liquid state, i.e. above the glass temperature, T_g, b and Cd increase with temperature. In the glassy state, we infer that Cd as well as b decrease during structural relaxation (physical aging). Different methods are considered to yield information about the correlation parameter, and the difficulties associated with the extraction of reliable values from the experimental data are outlined. Thus, the influence of the sub-T_g relaxation process and temperature-dependent distribution effects are discussed.

Introduction

The family of the para-substituted polyaryls have been the subject of particular interest in the quest of establishing relations between chemical and microstructural characteristics of polymers and their static and dynamic properties.[1-5] The common chemical structure of this group of polymers is $[-Ph-X-]_n$ where X can be O, CO, S, SO_2, CH_2, CO_3, etc., and Ph is an aromatic unit. Some typical examples are the polycarbonate of Bisphenol A (BPA-PC), poly(phenylene sulfide) (PPS), poly(aryl ether sulfone) (PES) and poly(aryl ether ether ketone) (PEEK). The latter, $[-Ph-O-Ph-O-Ph-CO-]_n$, is an aromatic thermoplastic semicrystalline polymer, often used as a high performance matrix for carbon fiber reinforced composites, like in APC2.[6] In the previous paper of this series,[7] the viscoelastic behavior of PEEK in various microstructural states was reported near the sub-T_g β relaxation. The aim of the present work is to extend this analysis near the glass transition in light of a model of "quasi punctual defects" (QPD model). The key points of the dynamic mechanical behavior of PEEK are listed in section I. The theoretical frame suitable for accounting for the main aspects of the results is discussed in section II. Then, the results are more extensively discussed in the frame of the QPD model in section III.

Experimental Section

The polymer used in this study bears the trademark PEEK 450G and was kindly supplied by ICI Inc., Wilton Research Centre (U.K.). As received samples are semicrystalline with a crystallinity ratio close to 34%. The average molecular weights are given to be $\overline{M}_n$ = 45 000 and $\overline{M}_w$ = 90 000. The amorphous state is obtained by heating the semicrystalline samples at 670 K and quenching the melt into cold water. During the quenching process, the samples were covered with an aluminum foil in order to avoid direct contact with water. The samples are obtained in the shape of thin platelets with the following dimensions: 0.5 × 2 × 14 mm^3.

Dynamic mechanical spectroscopy was performed by means of a homemade high resolution automated inverted pendulum,[8,9] specifically designed to study small samples like films and fibers. It measures the complex shear modulus $G^* = G' + iG'' = G_{real} + iG_{imag}$ as a function of temperature and frequency. $\tan(\Phi)$ will of course be referred to as the ratio G_{imag}/G_{real}.

The temperature scans (isochronals) are performed by increasing the temperature from 300 K up to 600 K at a rate of 1 K/min using one or several measurement frequencies. The frequency scans (isothermal scans) are carried out by decreasing the frequency from 1 Hz down to 0.0001 Hz at a fixed temperature.

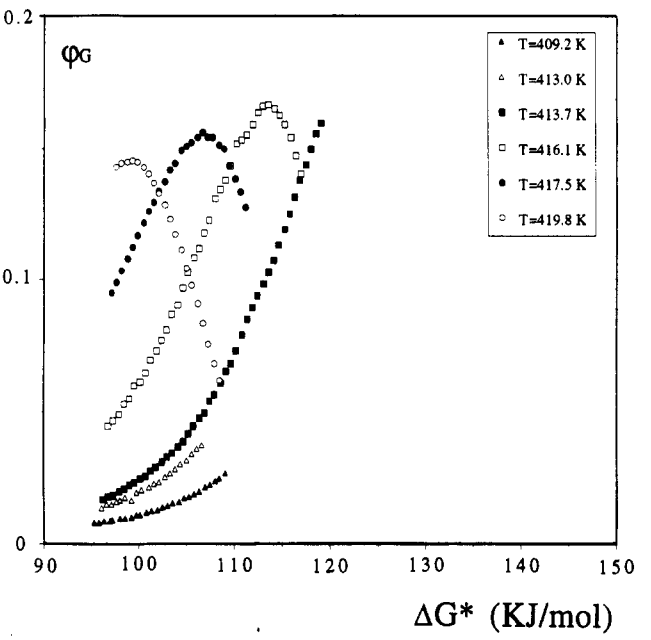

Figure 1. Distribution of the free activation enthalpy according to the Eyring equation. The scattering of the data exhibits the cooperative feature of the α relaxation in PEEK. The apparent activation entropy ΔS^* is positive and significantly different from zero.

I. Main Features of the Relaxation Phenomena near the Glass Transition

Apparent Activation Parameters of the α Relaxation of Amorphous PEEK. A simple approach for the characterization of the main relaxation process is to determine the values of the activation parameters. To this end, the apparent activation enthalpy and entropy of the relaxation associated with the glass transition are deduced according to the Eyring–Starkweather procedure.[10-14]

0024-9297/93/2226-4489$04.00/0

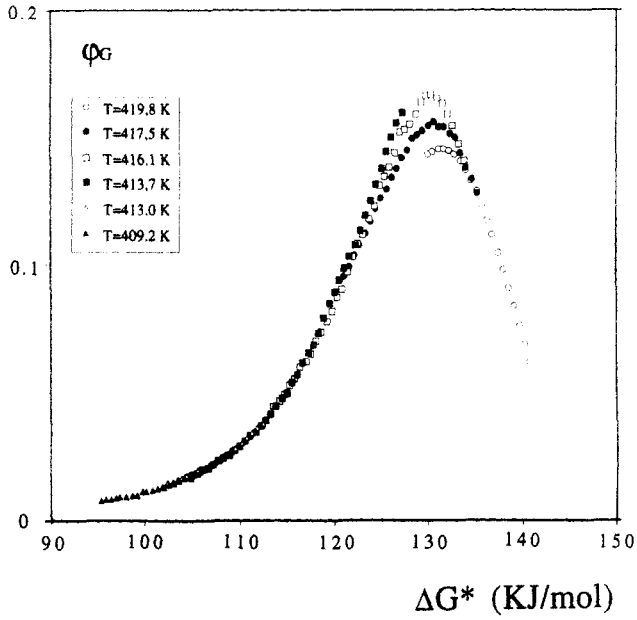

Figure 2. Distribution of the free enthalpy according to the Eyring equation, after the shifts along the energy axis. The shift factor gives an apparent activation entropy ΔS^* close to 3900 J/mol, which is unrealistically large for a microscopic event.

According to Eyring's rate theory, the characteristic frequency f of a relaxation process is

$$f = (kT/2\pi h) \exp(-\Delta H^*/RT) \exp(\Delta S^*/R)$$

$\Delta G^* = \Delta H^* - T\Delta S^*$ is the apparent activation free enthalpy and ΔH^* and ΔS^* are the activation enthalpy and entropy, respectively.

ΔG^* can also be written as

$$\Delta G^* = RT\, ln(kT/2\pi hf)$$

The relaxation spectrum is obtained according to

$$\varphi_G = \frac{2G''}{\pi(G_u - G_r)}$$

This description assumes uncorrelated microscopic events, represented by a generalized Maxwell model. For each value of T and f, it is possible to calculate φ_G and ΔG^*. The apparent distribution is obtained experimentally thanks to a series of isothermal runs in the temperature range extending from 409 to 415 K. Nevertheless, in order to build a common pattern, it is necessary to shift the isothermal curves along the ΔG^* axis (see Figures 1 and 2). The energy shift factors are used to evaluate the activation entropy according to

$$\text{cumulated shift factor} = C_{sf} = T\delta S^* + C_0$$

where C_0 is a constant. C_{sf} appears to be a linear function of T above 409 K. Thus,

$$\Delta S^* = \frac{dC_{sf}}{dT} = 3900 \text{ J/(K mol)}$$

The Starkweather treatment of the α process in amorphous PEEK clearly makes it evident that this mechanical relaxation is cooperative, because the pattern in Figure 1 is largely scattered.[10,11] The large value found for the ΔS^* parameter has of course no physical meaning, but it can be compared with the value obtained by Starkweather in Bisphenol A polycarbonate (BPA-PC) close to 2120 J/(K mol), which is again unrealistically large.[13] According to Starkweather, these high values for ΔS^* (and apparent activation energies, E_a) reflect "distributions of internal motions that are sampled differently at different temperatures".[14] More generally, the para-substituted polymers seem to present particularly large apparent activation energies and entropies. This will be related to the "fragile" behavior of aromatic molecular liquids as discussed by Angell.[15] We believe that the very high values of the activation parameters are a consequence of the cooperative

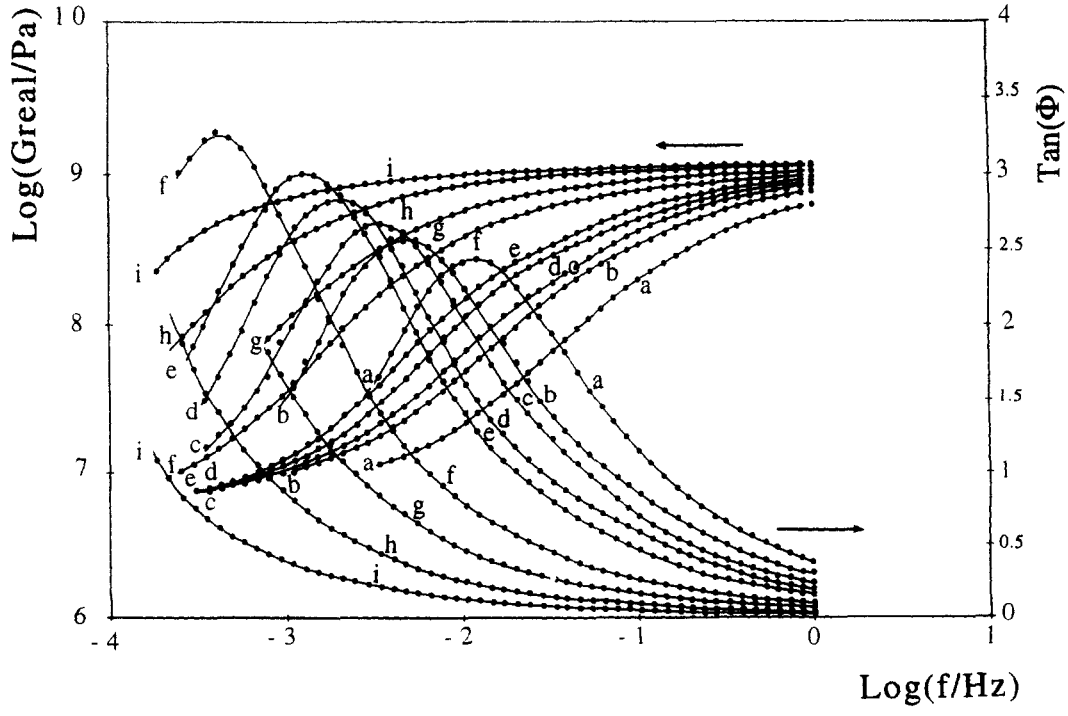

Figure 3. Isothermal curves of tan(Φ) and G_{real} = Re(G^*) versus log(f/Hz). The plots exhibit a departure from thermo-rheological simplicity because the maximum of tan(Φ) decreases with increasing temperature. The letters (a–i) refer to the following temperatures: (a) 421.17 K; (b) 420.42 K; (c) 419.67 K; (d) 419.42 K; (e) 418.92 K; (f) 418.17 K; (g) 416.66 K; (h) 415.91 K; (i) 415.16 K.

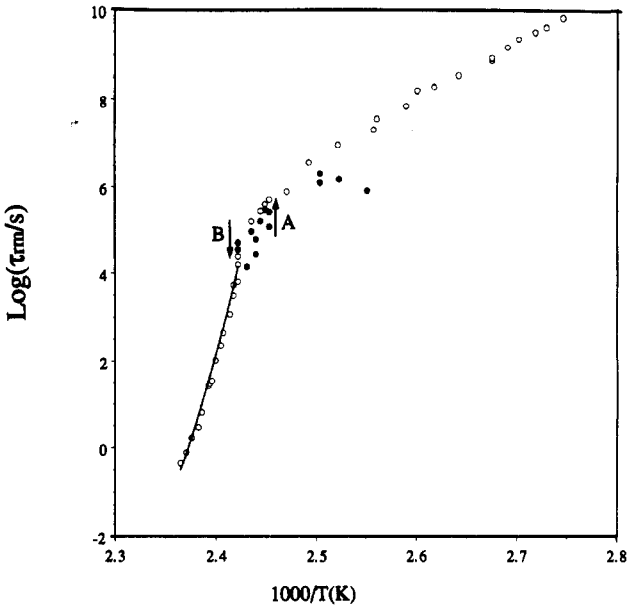

Figure 4. Evolution of the mechanical relaxation time τ_{rm} with temperature. The dark circles display the isothermal runs during which structural relaxation occurred. The empty circles display the isothermal runs during which structural relaxation can be neglected. At low temperature, an Arrhenius behavior is observed in the glassy state. Above T_g (412.5 K), b varies with temperature which causes the usual concave pattern of the WLF law. The solid line displays the result calculated from eq 6a using $t_0 = 3 \times 10^{-14}$ s, $\tau_0 = 10^{-13}$ s, $E_\beta = 43$ kJ/mol, and $\tau(1) = \tau_\beta = \tau_0 \exp(E_\beta/RT)$. The arrows display the evolution of τ_{rm} resulting from isothermal microscopic microstructural changes which occurred in order to reach a state (either equilibrium or isostructural) where the variations of Cd, b, and thus τ_{rm} become negligible during the time of the experiment (empty circles).

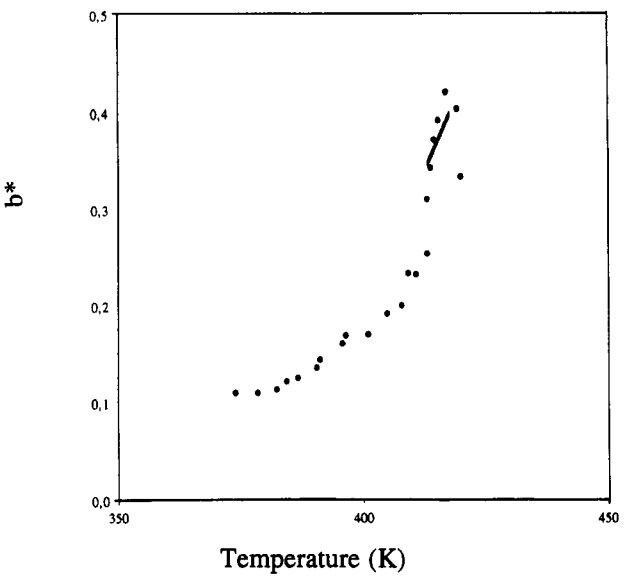

Figure 6. Estimation of the correlation parameter b according to the slopes of the log(tan(Φ)) vs log(f) plots for a series of isothermals in the temperature range from 370 to 421 K. The low temperature values are surprisingly low. This results from the influence of the β relaxation process and temperature dependent distribution effects. The solid line displays the result of eq 6a.

and hierarchically constrained dynamics of the glas transition.[16-18] In that case, the ΔG^* distribution obtained according to the Starkweather method is only apparent, because the calculation of this distribution implies a process based on a set of independent, unrelated microscopic events, which is unrealistic in the case of complex relaxing systems like disordered matter near the glass transition.

Thermo-Rheological Complexity. Figure 3 displays a series of isothermal curves obtained in the temperature range from 415 to 422 K. In linear scales, it is clear that the tan(Φ) vs log(f) plots cannot be shifted to form a single pattern. This was already noticed in the φ_G vs ΔG^* plots of Figures 1 and 2. The maximum of tan(Φ) decreases with increasing temperature. This feature is not resticted to the p-phenylene polymers, as we also observed a similar behavior for other amorphous polymers (such as atactic polystyrene). This effect was observed in amorphous PEEK on different series of isothermal runs, obtained either by increasing or decreasing the temperature. Thus it is not due to a crystallization process but it appears to be a characteristic of the glass transition in high molecular weight polymers.

Double Asymptotic Behavior of the Complex Shear Modulus. Figure 5 displays the Cole–Cole plot for amorphous PEEK and shows the two extreme asymptotic behaviors at low and high frequencies. At high frequencies, the droplike diagram exhibits a slope $(-\partial G''/\partial G'|_{\omega\to\infty})$ which usually lies in the range 0.3–1 for amorphous polymers. In the low frequency side, the slope $(\partial G''/\partial G'|_{\omega\to 0})$ is higher than the slope of the high frequency side. In the case of molecular glass forming systems, the low frequency slope approaches infinity.[19] In the case of polymers, the value is found smaller and usually lies in the range 2 to several units.

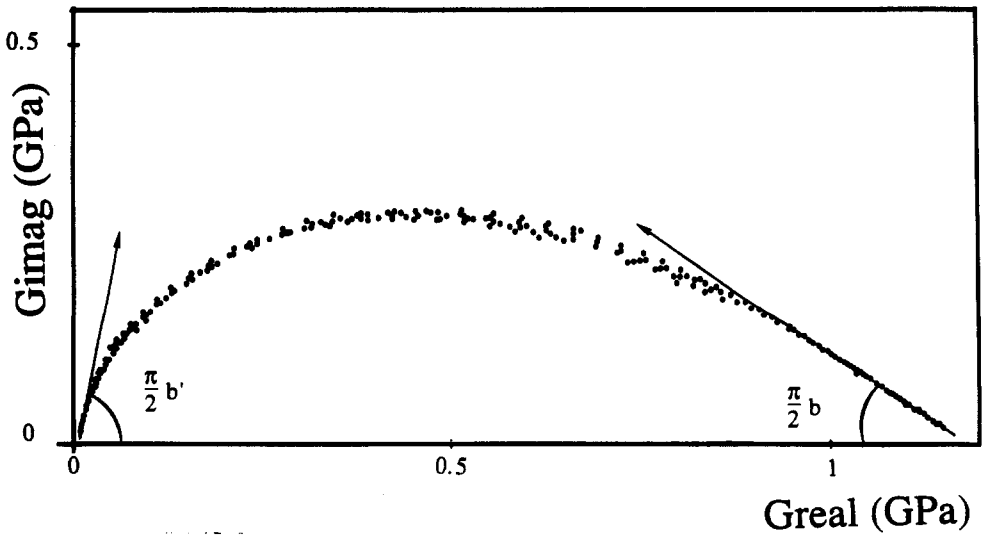

Figure 5. Cole–Cole plot of amporphous PEEK 450G. The arrows display the slopes leading to the values of b and b'.

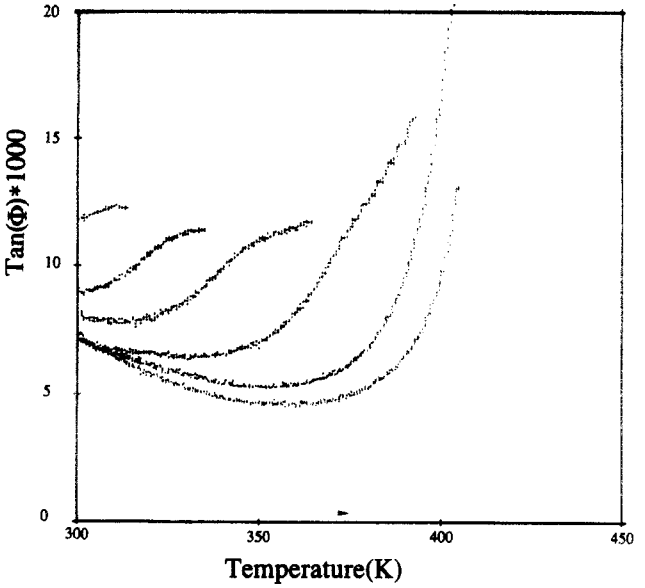

Figure 7. Successive heating isochronals at 1 Hz and at a rate of 1 K/min. A typical shoulder due to the excess of defects is clearly defined on the first isochronals.

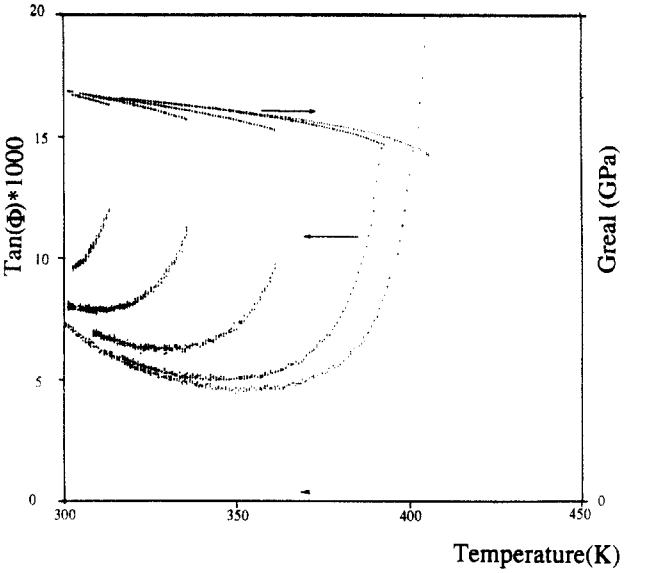

Figure 8. Cooling isochronals at 1 Hz obtained by decreasing the temperature after the heating scans of Figure 7.

Dependence of the Characteristic Relaxation Time on Microstructure. Figure 7 displays the evolution of tan(Φ) during successive heating isochronal scans (at 1 K/min and 1 Hz) for an amorphous sample freshly quenched and stored in liquid nitrogen for 24 h in order to avoid structural relaxation at room temperature. Nevertheless the sample has been kept at room temperature (T = 297 K) for about 20 min before experiment, a duration necessary to take it away from the quenching bath, remove aluminum protection, and proceed to the installation of the sample in the spectrometer. It can be observed that the successive heating scans do not fall on a single pattern, which indicates that a microstructural change in the material has occurred. The first, second, third and fourth isochronal curves exhibit an increase of tan(Φ) with temperature presenting a shoulder. This shoulder becomes less resolved on the fourth run and almost vanishes on the following ones. The temperature at which the shoulder appears is increased for the successive heating isochronal runs and is located close to the maximum temperature of the last previous run. Figure 8 shows the evolution of tan(Φ) (at 1 Hz) during the cooling scans occurring after each heating isochronal run of Figure 7. The effect of structural relaxation can also be observed, as it results in a gradual decrease of tan(Φ) for the successive scans. It can be seen that the values of tan(Φ) measured during a cooling isochronal run are always lower than the values recorded during the previous heating scan. Meanwhile, no shoulder can be observed. These results clearly show that the dynamic mechanical behavior of PEEK (as well as noncrystalline material more generally) is sensitive to the microstructural state. The evolution of tan(Φ) not only is a function of temperature but also changes with time according to a kinetics which is to be predicted. This nonlinear behavior is likely to be due to a change in the mechanical relaxation time, but changes in the relaxation function are not excluded.

II. Theoretical Approach of Molecular Mobility near T_g

General Aspects. In view of the complex features of the glass transition relaxation, namely (i) the inadequacy of the Arrhenius or Eyring relation to bring a physical description of the main (so called α) relaxation, (ii) the nonlinearity related to the evolution of the relaxation time with microstructure, (iii) thermo-rheological complexity, (iv) double asymptotic behavior (high and low frequency limits) of the complex shear modulus, it is necessary to find a frame of analysis yielding a coherent physical picture for all these experimental facts. As reviewed by Scherer[20] and others,[18,21] numerous papers have been devoted to the relaxation process associated with the glass transition. In spite of the success of the free volume approach,[22] the theory of Adam and Gibbs,[23] and the more recent mode coupling theories,[24] all of these models seem to find to find limits of applicability for the physical interpretation of the collective experimental features summarized above.[21] With this in mind, we propose to consider an alternative approach based on physical concepts involving parameters connected to the microstructure of disordered matter. An attempt was made to identify the degrees of freedom involved. In so doing, the limits of applicability of these concepts are restricted to the field of molecular mobility related to the main relaxation, as probed by dynamic mechanical spectroscopy and differential scanning calorimetry. This microscopic model has been developed in details elsewhere,[16-18] and the main features of it are presented here for the reader's convenience.

Quasi Punctual Defect Model. The amorphous matter is assumed to consist of close packed structural units (i.e. entities of the size of an aromatic ring, with an ether or ketone linkage in the case of PEEK). However, spatio-temporal density microfluctuations are well established to exist in the liquid. These microheterogeneities are also present in the glass below T_g but in a frozen-in state.[25-28] Thus, in this close arrangement, the disorder is not distributed uniformly at a microscopic level, but is taken into account by sites of disorder involving a few structural units in a weaker van der Waals interaction, and is thus believed to cause a local increase of enthalpy and entropy. If ΔH_f and ΔS_f are the enthalpy and the entropy of formation of 1 mol of defects respectively, then the equilibrium value of Cd is deduced from the Boltzmann equation:

$$Cd(t=\infty;T) = \frac{1}{1 + \exp(-\Delta S_f/R)\exp(\Delta H_f/RT)} \quad (1)$$

ΔS_f and ΔH_f can be estimated experimentally by calorimetric measurements.[29] Below T_g, Cd is time and tem-

perature dependent and is given by a kinetic equation, as will be seen below.

The molecular mobility is described by a time characteristic of the motions of the structural units. Part of the description of the correlated motions of these units has been formalized by Palmer et al.[30] in the frame of constrained dynamics. Following these authors, the disordered matter is represented by degrees of freedom of Ising spins, hierarchically distributed on levels. Due to the successive conditions imposed on the moving species, the characteristic time for reorganization at level n,$\tau(n)$, increases with n (i.e. with time) and can be written as[30]

$$\tau(n) = \tau(1)F(n)$$

where F is a function of the level n and the hierarchical condition. In the frame of this approach, an alternative to the formalism of Palmer *et al.* leads to a new expression for the function F, involving parameters related to the microstructural state of disordered matter. Thus the relaxation process is described[16] by a time dependent relaxation time $\tau(t)$ defined as follows:

$$\tau(t) = \tau(1) \qquad \text{for } t \le \tau(1)$$

$$\tau(t) = \tau(1)F(t,b) = \tau(1)\left(\frac{t}{t_0}\right)^{1-b} \qquad \text{for } \tau 1 < t < \tau_{max} \qquad (2)$$

$$\tau(t) = \tau_{max} \qquad \text{for } t \ge \tau_{max} \qquad (3)$$

The limit condition [3] yields the characteristic time for the whole process:

$$\tau_{max} = \left(\frac{\tau(1)}{t_0^{1-b}}\right)^{1/b}$$

where $b \in [0; 1]$ reflects the strength of the correlation between the degrees of freedom of the structural units: if b is near 0, the correlation is high and if b is close to 1, then the correlation effect is weak (in this case, the relaxation time $\tau(t)$ remains equal to $\tau(1)$). $\tau(1)$ is the time characteristic of the primary motion, and t_0 is a scaling parameter. This set of equations can be compared with

$$W(t) = W_0 \qquad \text{if } \omega_c t < 1$$

$$W(t) = W_0(\omega_c t)^{-n} \qquad \text{if } \omega_c t > 1 \qquad (4)$$

with the effective relaxation time $\tau^* = ((1-n)\omega_c^n/W_0)^{1/(1-n)}$ of the coupling model developed by Ngai and co-workers[31] (n and ω_c could be respectively similar to $1 - b$, and $1/t_0$). In spite of these apparent similarities, the conceptual bases of the coupling and QDP models are different. Moreover, in the QPD frame, the time $\tau(1)$ is assumed to reflect the most elementary motions, the combination of which can lead to translational motion, identified to the degrees of freedom giving rise to the β relaxation process. In fact, the coupling model does not address the molecular origin of the primary process.[32]

The dynamic mechanical behavior can be derived from the characteristic time for molecular motions near the glass transition. If a stress is applied on an amorphous material, the primary motions (with time $\tau(1)$) preferentially induce rearrangements in some of the defects. As long as the stress is maintained, the activated defects expand, and form sheared microdomains (the SMDs). This occurs via the above assumed correlated and hierarchically constrained motions and therefore with time $\tau_1(t)$ obeying eqs 2 and 3. If the stress is maintained for a longer time, then the next nearest SMD collapse and the Somigliana dislocations bordering them annihilate, yielding plastic strain. The time $\tau_2(t)$ characteristic of the plastic, non recoverable deformation process could again be given by an equation of the form[16] $\tau_2 = \tau(2)(t/t_0)^{1-b'}$.

After the successive molecular rearrangements resulting in the formation of a SMD, the local microstructure of the polymer chains must have changed and the correlation effects increase with the tendency of local chain alignment induced by shear. Moreover, the plastic inter-SMD reorganizations should involve a molecular mobility over a longer distance than that of the first intra-SMD correlated motions. As a consequence, the value of the correlation parameter b' is very sensitive to (decreases with) the presence of nodes, cross-links, or entanglements in the polymer. In the case of molecular glasses, all these chain-related effects vanish, and the value of the correlation parameter b' is close to unity.[19] The appendix of ref 16 shows how the kinetic evolution of activated defects, as stress is maintained, can be used to evaluate the time dependent compliance. After an approximate Laplace–Carson transform, this calculation leads to the frequency-domain response:

$$G^* = G_r + \frac{G_u - G_r}{1 + (i\omega\tau_{rm})^{-b} + H(i\omega\tau_{rm})^{-b'}} \qquad (5)$$

Where G_u is the unrelaxed modulus, G_r is the relaxed modulus, b and b' are the correlation parameters ($b < b' < 1$), H is a quantity close to unity, τ_{rm} is the mechanical relaxation time close to τ_{max},[16,21] and $\omega = 2\pi f$ is the angular frequency of the stress.

The phenomenological interest of the form of eq 5 is well-known, but the QPD model yields a physical meaning to it. At a molecular level, the nonelastic strain is not a consequence of the motions restricted within the defects but results from the expansion and annihilation of the SMDs as a whole, i.e. motions expanding over distances which could be several orders of magnitude larger than the characteristic length of the very local density fluctuations, which in turn are typically[25–27] of the order of $(0.5\ \text{nm})^3$. The size of the defects sites rather corresponds to the size of the local motions, giving rise to the elementary processes.

The QPD model accounts for the effect of the microstructure of amorphous media on the molecular mobility through the correlation parameter b assumed to be an explicit function of Cd. In so doing, in the liquid state, a decrease of the correlation effects with temperature is expected, implying in turn the evolution of τ_{rm} with temperature, as will be reported and discussed in the following section.

III. Discussion

QPD Model Analysis. It can be shown by numerical simulation that the value of the maximum of $\tan(\Phi)$ is nearly independent of b, but it is sensitive to the value of b' and G_r. Thus, the decrease of the maximum of $\tan(\Phi)$ from 3.2 at 419 K down to 2.5 at 421 K could be related to a decrease of b'. The physical meaning for this temperature dependence of b' is not clearly understood at the present time. Nevertheless, despite this nonabsolute thermorheological simplicity, a master curve can be built with a good approximation according to the relaxation times shown in Figure 4. The dark circles display the isothermal runs during which structural relaxation occurred in the glassy state. The empty circles show the location of isothermal runs for which two successive frequency scans give superimposed curves (i.e. for which

no significant structural relaxation occurred). This situation occurs either by a decrease or an increase of the relaxation time, at low temperatures (A) or at higher temperatures (B), respectively.

Correlation Parameter *b* in the Metastable Liquid State. Above 411 K, in the metastable equilibrium state, the plot exhibits a departure from the Arrhenian behavior, i.e. usual WLF-like pattern. The apparent activation energy is particularly high in that region (up to 1700 kJ/mol), with of course no physical meaning, as previously discussed. In this temperature range, the characteristic relaxation time τ_{rs} (see eq 7 below) is short, so that Cd reaches almost instantaneously its equilibrium value $Cd(t=\infty;T)$ which depends on temperature (eq 1). Therefore, the point here is to explain the evolution of b with Cd or, alternatively, with temperature. A simple way to evalaute experimentally the correlation parameters is based on the examination of the Cole–Cole diagram[16] (Figure 5). The high and low frequency limit values of the slopes in the droplike diagram lead to b and b', respectively, at one temperature (see eq 5 according to the relations

$$\left.\frac{\partial G''}{\partial G'}\right|_{\omega\to\infty} = -\tan\left(b\frac{\pi}{2}\right)$$

$$\left.\frac{\partial G''}{\partial G'}\right|_{\omega\to 0} = \tan\left(b'\frac{\pi}{2}\right)$$

It is measured that b is close to 0.36 ± 0.01 at 410 K and b' is near 0.88 ± 0.02 at 418 K. A second step further is the adjustment of the WLF-like part of the plot of $\log(\tau_{rm})$ versus reciprocal temperature. An explicit dependence of b with Cd can be expressed empirically as

$$b = \frac{1}{1 + a_1 \exp(-a_2 Cd)} \tag{6a}$$

This form is not unique, but this equation accounts for fast variations generally observed near T_g and for extreme cases where the equilibrium value of b is close to 1 when $Cd = 1$ (correlation effects vanish) and b is close to 0 when $Cd = 0$ (correlation effects are maximum in close packed matter). Moreover, a similar alternative equation for (6a) in the equilibrium state is

$$b = \frac{1}{1 + a'_1 \exp(-a'_2 T)} \tag{6b}$$

A reasonable fit is found for $a'_1 = 7.52 \times 10^8$, $a'_2 = 0.048$ K^{-1}, using $t_0 = 3 \times 10^{-4}$ s, $\tau_0 = 10^{-13}$ s, $E_\beta = 43$ kJ/mol, and $\tau(1) = \tau_\beta = \tau_0 \exp(E_\beta/RT)$. With this choice of parameters, the evolution of b with temperature is almost linear with temperature (db/dT is close to 0.011 K^{-1}). The a'_1 value results from that of a'_2 and the value of b at one temperature (from the use of the Cole–Cole plot, for example). The result is shown by the solid line on Figure 4. The parameters a'_2 and a'_1 are related to the dependence of b with temperature above T_g. A large value for these parameters would correspond to a liquid for which the relaxation time or viscosity drastically decreases with increasing temperature just above T_g, as it is the case for "fragile liquids" as defined by Angell.[15] This results in very high apparent activation energies and entropies, in agreement with the Eyring–Starkweather analysis presented above. Thus, db/dT, a'_1, and a'_2 could be considered as "fragility" parameters.

Although they are phenomenological in their form, eqs 6a and 6b represent the basic relations between microstructure (i.e. concentrations of defective sites of disordered matter) and molecular mobility (i.e. the correlation parameter b in eq 4). Actually, eq 6a explicitly reflects the decrease of the correlation effects (increase of b) with increasing Cd. Alternatively, the possible changes in the coupling parameter versus temperature in the liquid state are also discussed by Ngai[33] assuming an increase of $1 - n$ (see eq 4) with increasing temperature.

Furthermore, eq 6a remains valid even if the system is out of equilibrium whereas eq 6b is only valid in the metastable equilibrium state and could be regarded as the phenomenological expression of eq 6a together with (1). Thus, we have determined the parameters of both eqs 6a and 6b in section III.

The third attempt to obtain more information on the value of b is the calculation of the slopes of the plots $\log(\tan(\Phi))$ versus $\log(f)$. It can be easily shown from eq 5 that $\partial\log(\tan(\Phi))/\partial\log(f) = b$ when $\omega\tau_{rm} \gg 1$. The values deduced from this procedure, hereafter called b^*, are plotted versus temperature on Figure 6. Above 418 K, it can be seen that b^* decreases with temperature but the condition $\omega\tau_{rm} \gg 1$ is no longer valid in our frequency window and b^* becomes different from b in this temperature range. Between 418 and 412 K, the values of b deduced by eq 6b fall in agreement with b^*.

Isostructural Glassy State. In order to reach the isostructural state, the samples of amorphous PEEK were annealed at 390 K for 72 h. In these conditions, further structural relaxation could be neglected. The phase loss levels in the low temperature part of the diagram of Figure 4 are of the order of $(2–5) \times 10^{-3}$ radians. After this thermal treatment, two successive isothermal runs yield the same result within experimental accuracy. Moreover, it was checked that no crystallization occurred during annealing at $T = T_g - 20$ K: before and after annealing, the $\tan(\Phi)$ vs T peak patterns at 1 Hz of freshly quenched and annealed samples are the same above 415 K, i.e. above T_g, in the metastable equilibrium liquid state. SAXS experiments also confirm the absence of crystallites.

Below 400 K, an Arrhenian behavior is obeyed (Figure 4), as the plot $\log(\tau_{rm})$ against reciprocal absolute temperature is a straight line. Nevertheless, between 400 and 410 K, the apparent activation energy increases and a slight departure from the Arrhenius behavior as the liquid state is approached can be observed. Moreover, although the exact value of the apparent activation energy in the isostructural state is difficult to evaluate with great accuracy because of the nonexact thermo-rheological simplicity, the apparent activation energy in the linear part of the curve can be estimated at about 250 kJ/mol. This value is too high to be given the physical meaning of a potential barier between two stable states of a structural unit. Nevertheless, as the Arrhenius law is obeyed in the isostructural state, the primary motions responsible for the α relaxation, with characteristic time $\tau(1)$, also exhibit an Arrhenius behavior like most of the subvitreous simple relaxations. The assumption that $\tau_\beta = \tau_0 \exp(E_\beta/RT) = \tau(1)$ implies[31–34] that the apparent activation energy for mechanical relaxation, $R\partial ln(\tau_{rm})/\partial(1/T) = E_\beta/b$ because b and Cd are constant in the isostructural state. This could explain the high value of the activation energy in this regime. Nevertheless, a correlation parameter b near 0.17 (±0.01) is expected below 400 K because the activation energy for the low temperature component of the secondary or so-called β transition in PEEK is close to 43 kJ/mol.[7] Of course, the fact that the microstructure is non temperature dependent shows that the defect concentration is no longer given by eq 1, which gives the equilibrium value $Cd(t=\infty;T)$ as a function of temperature (the system is clearly out of equilibrium). The kinetics of the return

toward equilibrium is considered in section III, where the microstructure of the glassy polymer leads to short characteristic times for structural relaxation.

To go a step further, the values of b^* evaluated in the isostructural state are displayed in Figure 6. In the low temperature range, b^* was expected to be constant but actually varies from 0.1 at 370 K to 0.17 at 400 K. These rather low values of b cannot be understood in the QPD correlation frame because the resulting apparent value of τ_{max}, given by eq 3, would then be of the order of 10^{24} s at 370 K. This high value is far from the order of magnitude of the mechanical relaxation time observed on the Arrhenius plot in Figure 4. A first effect could result from the merging of the high temperature tail of the β process with the onset of the α relaxation, even if the maximum of the β relaxation is located, at 1 Hz, near 185 K.[7] The plots of $\log(\tan(\Phi))$ versus $\log(f)$ then result from opposite tendencies due to the presence of the sub-T_g relaxation process and of course the glass transition relaxation. This could explain why b^* is not constant in the temperature range from 370 K up to 400 K.

Furthermore, the low values of b in the glassy state at temperatures far below T_g have also been shown to be related to distribution effects.[35] If the time $\tau(1)$ is distributed, then the result is a low apparent value for b, sometimes lower than 0.1. Another possibility deals with the spatial distribution of the defect concentration (i.e. of parameter b) that is believed to induce the presence of regions of high and low cooperativity. Moreover, it is easy to show (see eq 4) that if the variable $1/b$ is distributed, then it is also the case for the variable $\ln(\tau_{max})$, and the variance of the variable $\ln(\tau_{max})$ is given by $\mathrm{var}(\ln(\tau_{max})) = [\ln(\tau(1)/t_0)]^2\mathrm{var}(1/b)$. This shows that the width of the distribution of the relaxation times τ_{max} increases with decreasing temperature. Thus, the ratio [var(ln(τ_{max})) at 300K]/[var(ln(τ_{max})) at 400 K] is close to 1.7. This results in a lower apparent value of b at low temperature, and the value of the fractional exponent of the KWW relaxation function can be interpreted in terms of a width parameter of the distribution of relaxation times related to the α process and/or a correlation parameter.[36] At higher temperatures, the distribution effects have a weaker influence on the KWW exponent. These extensions of the model for the molecular mobility in terms of distributions lead naturally to a multiorder parameter description, which is also necessary to explain memory effects usually observed through DSC or dilatometric measurements, as shown by Kovacs and many others,[37] and more generally to account for the value of the Prigogine–Defay ratio greater than unity at T_g.[38] Therefore, the fractional exponent of the stretched exponential results first from the hierarchical constraint dynamics of the glass transition (see section I) and its value is affected by the temperature dependent effects of the distributions of b and/or $\tau(1)$. As a consequence, the value of b^* depends on (i) the apparent value of b and (ii) the influence of the higher temperature tail of the sub-T_g relaxation.

Following is a short discussion about the identification of $\tau(1)$ from τ_β. If $\tau(1)$ is considered to be different from τ_β, then an activation energy for the primary process of the order of 85 kJ/mol is necessary, assuming a model with no distribution. Distribution-free numerical simulations can be carried out with success to explain the evolution of the viscoelastic response with temperature and defect concentration, after an adequate choice for t_0. This assumption would bring a phenomenological character to this analysis. Indeed, if the activation energy for the noncooperative primary process was 85 kJ/mol, then the maximum of the $\tan(\Phi)$ peak should be close to T = 350 K at 1 Hz, assuming the Debye frequency as the preexponential factor for $1/\tau(1)$. As a matter of fact, there is no relaxation close to this frequency–temperature window, which rules out any molecular interpretation of the primary process.

Physical Aging. Some Theoretical Aspects of Structural Relaxation in the QPD Frame. The main features of structural relaxation in the frame of the QPD model will be briefly recalled here. The time τ_{mol} is referred to as the characteristic time for the displacement of a few structural units (arranged to form a defective site) over a length characteristic of their collective size. This characteristic time is identified to τ_{max} and falls not far from τ_{rm}.[18,21] The modeling for structural relaxation is based on the assumption that the defects can diffuse and reorganize according to[39]

$$d^+ + d^- \leftrightarrow 2d^0 + 2(\Delta H_f - T\Delta S_f)$$

where d^+ and d^-, respectively, refer to high density and low density defects and d^0 is a normal site, with no defect.

Thus, the defect concentration is time dependent according to the nonlinear kinetic equation

$$\frac{dCd}{dt} = \frac{Cd(t) - Cd(t=\infty;T)}{\tau_{rs}} \tag{7}$$

τ_{rs} is the characteristic time for structural relaxation, of the order of magnitude of

$$(Cd)^{-2/3}\tau_{mol} \approx (Cd)^{-2/3}\tau_{rm} \approx (Cd)^{-2/3}\left(\frac{\tau(1)}{t_0^{1-b}}\right)^{1/b} \tag{8}$$

with b considered a function of Cd. The exponent $-2/3$ results from the hypothesis that the defects are located on a cubic pseudolattice. It is possible to solve numerically eq 7 by the fourth order Runge–Kutta method.[40]

The modeling presented above accounts for the main features of the relaxation processes occuring near or below T_g. Nevertheless, it is well-known that the glass transition phenonenon implies a multiple order parameter description. In agreement with this remark, it was previously shown that a description associated with a distribution of parameters like the correlation parameter b (and/or ΔH_f and ΔS_f) was necessary to explain the evolution of the defect concentration as observed by calorimetry.[39] This spatial distribution of the correlation parameter could be regarded as reflecting fluctuations of defect concentration, with a larger characteristic length. Thus, the density microfluctuations in disordered matter appear at a local scale at the level of defective sites but also at a longer correlation length with fluctuations of Cd. This description is in close agreement with the different scales of fluctuations as revealed by quasi elastic light scattering experiments.[41] In the field of mechanical spectroscopy, the calculation of mechanical coupling among regions of different defect concentrations and different viscoelastic behavior is not a straightforward task. We show in this section that a simple description, with only one type of defect, can be used enough to account satisfactorily for most of the experimental features.

Experimental Results during Isochronal Experiments. The existence of a shoulder on the low temperature tail of the α process in PEEK observed on heating has already been described,[42] as well as in other polymers, for example in PES,[43,44] BPA-PC,[45,46] and PMMA.[21] It is attributed to the presence of a high disorder site concentration within the glassy polymer. Nevertheless, this effect has to be not considered as a true relaxation phenomenon.

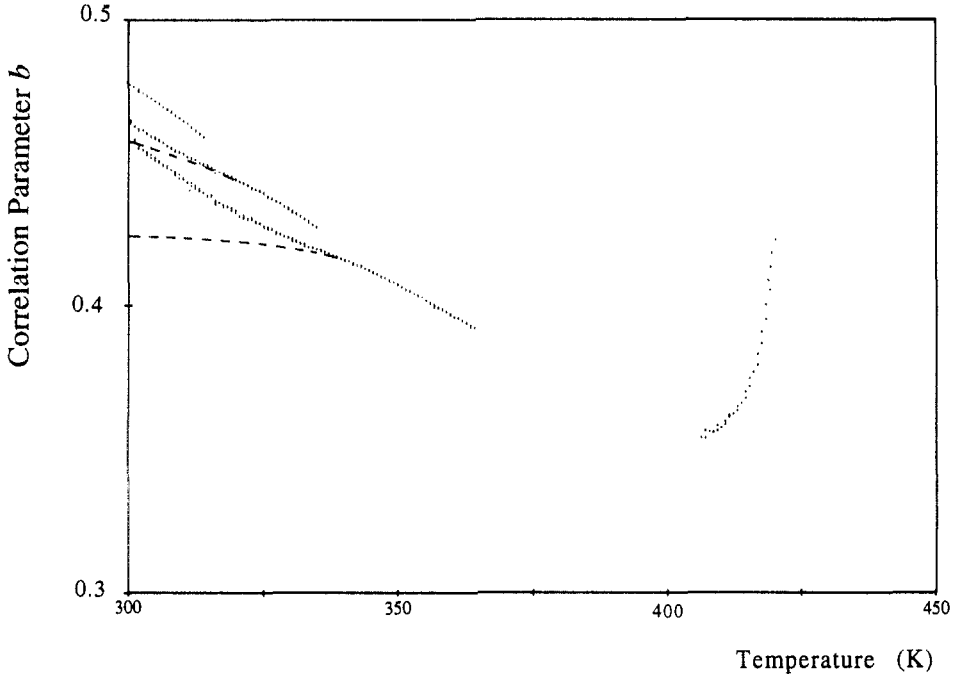

Figure 9. Evolution of b with temperature during heating isochronals. The three low temperature curves (below 275 K) have been obtained from the three first isochronals of Figure 7. Note the increasing influence of the β relaxation process which results in higher apparent values for b at low temperature. The supposed evolution of b is displayed as dashed lines. Above 400 K, b increases with temperature because the material is in the metastable equilibrium state.

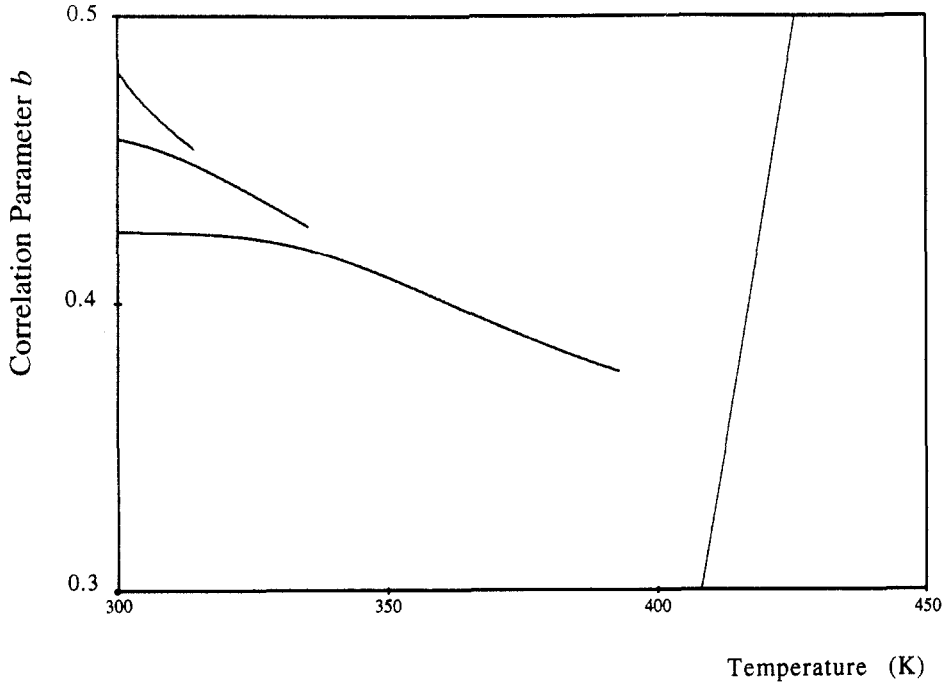

Figure 10. Numerical simulation of the experimental results of Figure 9. The first three curves result from eq 7 with a 600-ms time increment and $\tau_n = 10(Cd)^{-2/3}(\tau(1)/t_0^{1-b})^{1/b}$, $\tau(1) = \tau_\beta = \tau_0 \exp(E_\beta/RT)$, $t_0 = 3 \times 10^{-14}$ s, $\tau_0 = 10^{-13}$ s, $E_\beta = 43$ kJ/mol, $b = [1 + a_1 \exp(-a_2 Cd(t=\infty;T))]^{-1}$ with $a_1 = 9432.7$ and $a_2 = 29$, $Cd(t=\infty;T) = [1 + \exp(-\Delta S_f/R) \exp(\Delta H_f/RT)]^{-1}$ with $\Delta H_f = 11.0$ kJ/mol and $\Delta S_f = 19.4$ J/(mol K), and $T = dT/dt\,t + T_0$ with $dT/dt = 1$ K/min and $T_0 = 300$ K. The initial defect concentration is determined from the initial value of b. The higher temperature curve, near the metastable state, results from eq 6b.

In the frame of the QPD model, it results from a defect concentration in excess. During the temperature scans, the molecular mobility increases (with temperature), which in turn causes the collapse of the defects according to eq 7 and in turn decreases the molecular mobility. This results in the shoulder pattern of tan(Φ) vs temperature. The key point now is to describe quantitatively the kinetics of this structural relaxation process during a heating scan. The evolution of Cd with time and temperature is calculated according to eq 7 and then used to account for the evolution of the correlation parameter b during a typical heating isochronal. Finally, the numerical simulation is compared with the values directly deduced from experiments.

Figure 9 displays the values of b deduced from the three first isochronal runs on heating (at 1 Hz) of Figure 7. For each temperature, an iterative dichotomous procedure is performed in order to calculate the loss factor tan(Φ) according to eq 5, and then the value of $b \in [0.05; 0.60]$ is obtained after 50 dichotomous steps. In order to account for the contribution of the β process to the value of tan(Φ), a subtraction of the phase loss is carried out according to

$\Delta\Phi$ (in milliradians) = $43.86 - 0.12691T - 2.2109 \times 10^{-4} T^2 + 6.6138 \times 10^{-7} T^3$ (for $T < 380$ K). Actually, the secondary relaxation contribution is rather difficult to remove exactly without the use of a high number of adjustable parameters, and $\Delta\Phi$ could be be considered to be a lower estimation of the sub-T_g component. Furthermore, the high temperature tail of this process is known to vary with microstructure. For example, it increases with annealing below T_g.[7] In the low temperature range, not far below T_g, the value of the correlation parameter b is found to decrease with increasing temperature. Again, this is due to diffusion and reorganization of disordered regions. Thus, the defect concentration decreases and this results in an increase of the correlation effects. The value of b reached at the end of an isochronal run should be close to the value of b at the beginning of the following run, because structural relaxation is negligible during the faster cooling isochronals. This prediction is not absolutely verified (Figure 9), probably because of the increasing influence of the β process. Nevertheless, the estimated variations of b with respect to temperature are displayed in dashed lines. Above 410 K, in the equilibrium state, the evolution of b with temperature is more usual and should be governed by eqs 1 and 6a, resulting in (6b). The almost linear increase of b with temperature is well observed. The simulated curves are shown as continuous lines in Figure 10. The low temperature curves were obtained by solving eq 7 with $\tau_{rs} = 10(Cd)^{-2/3}\tau_{rm}$ (see eq 8). The high temperature simulation line displays the value of b deduced from eq 6b. Experimental points and simulated curves are in good agreement. At high temperatures, the evolution of b is independent of the initial value and only depends on the ratio $\tau_{rs}/(Cd)^{-2/3}\tau_{rm}$. Nevertheless, the temperature at which a given curve joins the common pattern does depend on the initial defect concentration. We believe that this is the basic reason for the evolution of the shift of the structural relaxation shoulder to higher temperatures.

Concluding Remarks

The aim of this work is to contribute to providing precise measurements of the visocelastic response of amorphous PEEK near the glass transition and to present a frame of analysis yielding a microscopic understanding of the dependence of the molecular mobility on the microstructural state of disordered matter (the DQP model).

In disordered matter, the local density fluctuations result in the formation of "weak" sites (the QPD) where the stress preferentially biases the molecule motions. The activated QPDs act as a "source of shear" and form microdomains of sheared material (the SMDs). Under the applied stress, the SMDs expand, and in the early stages this results in recoverable anelastic strain. When the SMDs collapse, the rearrangements induce plastic strain. Both processes involve correlated and hierarchically constrained motions (eqs 2 and 3). This leads to the complex shear modulus as given by eq 5. Above T_g, the system is in equilibrium, as Cd reaches quasi instantaneously its metastable equilibrium value (eq 1). Below T_g, the system is out of equilibrium and Cd remains constant at temperatures far below T_g or changes with time according to a kinetics which leads to the description of structural relaxation. The correlation parameter b is a function of Cd, accounting for the dependence of the molecular mobility on the microstructure of the amorphous matter. The QPD model thus accounts for the microscopic aspects related to microfluctuations in density or intermolecular cohesive forces which are present in the liquid as well as in the glassy states. Moreover, it is shown that a single KWW relaxation function does not yield a satisfactory description of the dynamic mechanical behavior of molecular and polymeric glasses in a wide frequency–time domain, but two correlation parameters (b and b') are necessary.

These original features of the QPD model contribute to show a difference from other approaches dealing with strongly interacting systems, like the coupling model as developed by Ngai and co-workers for example. The QPD model establishes a relation between calorimetric properties related to structural relaxation and dynamic behavior. An attempt was made to identify the nature of the microscopic events connected to the glass transition relaxation as probed by dynamic mechanical spectroscopy. The atomic motions yielding this dynamic behavior involve rearrangements with translational character and the concept of Somigliana lines, which implicitly restricts this approach to the dynamic response of disordered matter submitted to a mechanical stress as the stimulus.

Acknowledgment. We are grateful to ICI Inc., Wilton Research Center (U.K.), for providing the sample of semicrystalline PEEK 450G. We also want to thank Pr. J. Perez for helpful comments on this paper.

References and Notes

(1) Jho, J. Y.; Yee, A. F. *Macromolecules* **1991**, *24*, 1905–1913.
(2) Dumais, J. J.; Cholli, A. L.; Jelinski, L. W.; Hedrick, J. L.; McGrath, J. E. *Macromolecules* **1986**, *19*, 1884–1889.
(3) Henrichs, P. M.; Nicely, V. A.; Fagerburg, D. R. *Macromolecules* **1991**, *24*, 4033–4037.
(4) Yee, A. F.; Smith, S. A. *Macromolecules* **1981**, *14*, 54–64.
(5) Schaefer, J.; Stejskal, E. O.; McKay, R. A.; Dixon, W. T. *Macromolecules* **1984**, *17*, 1479–1489. See also: Schaefer, J.; Stejskal, E. O.; Perchak, D.; Skolnick, J.; Yaris, R.; *Macromolecules* **1985**, *18*, 368–373.
(6) Blundell, D. J.; Osborn, B. N. *Polymer* **1983**, *24*, 953–958. See also: Dawson, P. C.; Blundell, D. J. *Polymer* **1980**, *21*, 577–578.
(7) David, L.; Etienne, S. *Macromolecules* **1992**, *25*, 4302–4308.
(8) Etienne, S. In *International Summer School on Mechanical Spectroscopy*, Krakow, Sept 1991. Magalas, L., Ed.; Elsevier: Amsterdam, 1993 (in press).
(9) Etienne, S.; Cavaille, J. Y.; Perez, J.; Point, R.; Salvia, M. *Rev. Sci. Instrum.* **1982**, *53*, 1261–1266.
(10) Starkweather, H. W., Jr. *Macromolecules* **1981**, *14*, 1277–1281.
(11) Starkweather, H. W., Jr. *Macromolecules* **1988**, *21*, 1798–1802.
(12) Starkweather, H. W., Jr. *Macromolecules* **1989**, *22*, 4060–4062.
(13) Starkweather, H. W., Jr. *Macromolecules* **1990**, *23*, 328–332.
(14) Starkweather, H. W., Jr. *Polymer* **1991**, *32* (13), 2443–2448.
(15) Angell, C. A. *J. Non-Cryst. Solids* **1991**, *131–133*, 13–31.
(16) Perez, J.; Cavaille, J. Y.; Etienne, S.; Jourdan, C. *Rev. Phys. Appl.* **1988**, *23*, 125–135.
(17) Perez, J. *Solid State Ionics* **1990**, *38*, 69–79.
(18) Perez, J. Physique et Mécanique des polymères amorphes, Technique et Documentation; Lavoisier: Paris 1992, (ISBN 2-85206-787-0).
(19) Sekkat, A. Thesis, Lyon, France, December 7, 1992.
(20) Sherer, G. W. *J. Non-Cryst. Solids* **1990**, *123*, 75–89.
(21) Etienne, S. *J. Phys. IV* **1992**, *2* (C2), 41–50.
(22) Cohen, N. H.; Grest, G. S. *Phys. Rev. B* **1979**, *20* (3), 1077–1098. See also: Grest, S. G.; Cohen, M. H. *Advances in Chemical Physics*; Pigogine, I., Rice, A., Eds.; Wiley: New York, Chichester, Brisbane, Toronto, 1989; Vol. 48, pp 455–526 (ISBN 0-471-08294-5).
(23) Adam, G.; Gibbs, J. H. *J. Chem. Phys.* **1965**, *43*, 139.
(24) Leutheusser, E. *Phys. Rev.* **1984**, *A29*, 2765. See also: Bengtzelius, U.; Goetze, U.; Sjoelander, A. *J. Phys.* **1984**, *C17*, 5915.
(25) Malhotra, B. D.; Pethrick, R. A. *Polym. Commun.* **1983**, *24*, 165–167.
(26) Curroe, J. J.; Roe, R. J. *Polymer* **1984**, *25*, 1424–1430.
(27) Victor, J. G.; Torkelson, J. M. *Macromolecules* **1987**, *20*, 2241–2250.
(28) Achibat, T.; Boukenter, A.; Duval, E.; Lorentz, G.; Etienne, S. *J. Chem. Phys. 95*, **1991**, 2949–2954.
(29) Perez, J. *Rev. Phys. Appl.* **1986**, *21*, 93–107.

(30) Palmer, R. C.; Stein, D. L.; Abrahams, E.; Anderson, P. N. *Phys. Rev. Lett.* **1984**, *53*, 958–961.
(31) Rendell, R. W.; Ngai, K.L. In *Relaxation in Complex Systems*; Ngai, K. L., Wright, G. B., Eds.; Office of Naval Research: Arlington, VA, 1984; pp 309–345 (available from the National Technical Information Service, U.S. Department of Commerce, 5285 Port Royal Road, Springfield, VA 22161).
(32) Ngai, K. L. *J. Non-Cryst. Solids* **1987**, *95–96*, 969–976.
(33) Ngai, K. L. *J. Non-Cryst. Solids* **1991**, *131–133*, 80–83.
(34) Ngai, K. L. *Comments Solid State Phys.* **1979**, *9* (4), 127–140.
(35) Etienne, S.; Cavaille, J. Y.; Perez, J. *J. Non-Cryst. Solids* **1991**, *131–133*, 66–70.
(36) Roy, A. K.; Jones, A. A.; Inglefield, P. T. *Macromolecules* **1986**, *19*, 1356–1362.
(37) Kovacs, A. J.; Aklonis, J. J.; Hutchinson, J. M.; Ramos, A. R. *J. Polym. Sci., Polym. Phys. Ed.* **1979**, *17*, 1907. See also: Struik, L. C. E. *J. Non-Cryst. Solids* **1991**, *131–133*, 395–407.
(38) Davies, R. O.; Jones, G. O. *Adv. Phys.* **1954**, *2*, 370.
(39) Perez, J. *Polymer* **1988**, *29*, 483–489.
(40) Press, W. H.; Flannery, B. P.; Teukolsky, S. A.; Vetterling, W. T. *Numerical Recipes in C, The Art of Scientific Computing*; Cambridge University Press: Cambridge, New York, New Rochelle, Melbourne, Sydney, 1988 pp 569–580 (see also references therein) (ISBN 0-521-35465-X).
(41) Fischer, E. W. In *Basic Features of the Glassy State*; Colmenero, J., Alegria, A., Eds.; Word Scientific: Teaneck, NJ, London, Hong-Kong, 1990; pp 172–191 (ISBN 981-222-0031-05).
(42) Sasuga, T.; Hagiwara, M. *Polymer* **1985**, *26*, 501–505. See also: Sasuga, T.; Hagiwara, M. *Polymer* **1986**, *27*, 821–826.
(43) Sasuga, T.; Hayakawa, N.; Yoshida, K. *J. Polym. Sci., Polym. Phys. Ed.* **1984**, *22*, 529–533.
(44) Fried, J. R.; Letton, A.; Welsh, W. J. *Polymer* **1990**, *31*, 1032–1037.
(45) G'Sell, C.; El Bari, H.; Perez, J.; Cavaille, J. Y.; Johari, G. P. *Mater. Sci. Eng.* **1989**, *A110*, 223–229.
(46) Bauwens-Crowet, C.; Bauwens, J.-C. *Polymer* **1990**, *31*, 646–650.